

Time and Energy Management During Approach A Human-in-the-Loop Study

de Jong, Paul; Bussink, F. J L; Verhoeven, RPM; de Gelder, N; van Paassen, Rene; Mulder, Max

DOI

[10.2514/1.C033741](https://doi.org/10.2514/1.C033741)

Publication date

2017

Document Version

Accepted author manuscript

Published in

Journal of Aircraft: devoted to aeronautical science and technology

Citation (APA)

de Jong, P., Bussink, F. J. L., Verhoeven, RPM., de Gelder, N., van Paassen, R., & Mulder, M. (2017). Time and Energy Management During Approach: A Human-in-the-Loop Study. *Journal of Aircraft: devoted to aeronautical science and technology*, 54(1), 177-189. <https://doi.org/10.2514/1.C033741>

Important note

To cite this publication, please use the final published version (if applicable).
Please check the document version above.

Copyright

Other than for strictly personal use, it is not permitted to download, forward or distribute the text or part of it, without the consent of the author(s) and/or copyright holder(s), unless the work is under an open content license such as Creative Commons.

Takedown policy

Please contact us and provide details if you believe this document breaches copyrights.
We will remove access to the work immediately and investigate your claim.

Time and Energy Management during Descent and Approach: A Human-in-the-Loop Study

P.M.A. de Jong*

Delft University of Technology, P.O. Box 5058, 2600 GB Delft, The Netherlands

F.J.L. Bussink[†] R.P.M. Verhoeven[‡] N. de Gelder[§]

National Aerospace Laboratory, P.O. Box 90502, 1006 BM Amsterdam, The Netherlands

M.M. van Paassen,[¶] M. Mulder^{||}

Delft University of Technology, P.O. Box 5058, 2600 GB Delft, The Netherlands

Time and Energy Managed Operations (TEMO) is a new integrated planning and guidance concept that optimizes the vertical aircraft trajectory, to achieve a continuous engine-idle descent whilst satisfying time constraints. To investigate acceptance of the concept and the influence of pilot involvement on performance, TEMO was evaluated in a real-time simulation involving nine airline pilots. Three Human-Machine Interface (HMI) variants were tested, these varied in the level of information presented. The results were compared to computer simulations with a zero-delay pilot response model, to evaluate the effect of pilot reaction time variation on performance and environmental impact. Results indicated that the effects of pilot response delays are limited. Pilots preferred the HMI variant that included a timer to support accurate selection of flaps and gear. Although

*PhD. student, section Control and Simulation, Faculty of Aerospace Engineering, Delft University of Technology, Kluyverweg 1, 2629 HS Delft, The Netherlands. AIAA Student Member. E-mail: p.m.a.dejong@tudelft.nl

[†]Medior Researcher, Cockpit and Flight Operations Division, National Aerospace Laboratory, Anthony Fokkerweg 2, 1059 CM Amsterdam, The Netherlands.

[‡]Senior Researcher, Cockpit and Flight Operations Division, National Aerospace Laboratory

[§]Senior Researcher, Cockpit and Flight Operations Division, National Aerospace Laboratory

[¶]Associate Professor, section Control and Simulation, Delft University of Technology, AIAA Senior Member

^{||}Professor, section Control and Simulation, Delft University of Technology, AIAA Associate Fellow

the timer did not significantly affect system performance, it did reduce variation in the pilot response. Results further indicated that modifications to the TEMO concept are possible to further improve time performance.

I. Introduction

The expected growth in air traffic,¹ combined with an increased public concern for the environment and higher fuel costs, forces the aerospace community to rethink the current air traffic system design. Both in the United States² and Europe,³ research projects have been initiated to develop the future Air Transportation System (ATS) to address capacity, environmental, safety and economic issues.

To address the environmental issues during descent and approach, a novel Continuous Descent Operations (CDO) concept,⁴ named Time and Energy Managed Operations (TEMO), has been developed.⁵ TEMO uses energy principles to reduce aircraft fuel burn, gaseous emissions and noise nuisance whilst maintaining runway capacity. TEMO differs from other CDO concepts⁶⁻¹² by explicitly using an energy management algorithm¹³ to achieve a continuous engine-idle descent, while satisfying time constraints at two control points, Initial Approach Fix (IAF) and the runway threshold.

When integrated in a capable Flight Management System (FMS) and autopilot, TEMO could in principle be used in full authority automation during the descent phase of flight. For two reasons, namely for facilitating a retrofit to current aircraft, and for optimizing the human-machine system, this paper considers a system that keeps the pilot in the loop. Previous flight deck automation-related research has shown that incorrect use of automation may lead to severe human performance problems,¹⁴⁻¹⁷ especially during unanticipated events that require human intervention.¹⁸ Due to the unanticipated variability in ‘open’ systems¹⁹ such as aircraft, there is always a role foreseen for human abilities, such as inductive reasoning and complex pattern matching, which still outperform computer design. A prerequisite for supporting the human contribution is to properly inform the pilot about the rationale that drives the automation.²⁰

In the research presented here, we consider a scenario where flap selections and gear deployment are performed by the pilot, and TEMO automation controls the auto-throttle and auto-speedbrake. We will investigate what and how much information should be presented to support pilots operating TEMO, to maintain high levels of performance. The paper discusses the results of a pilot-in-the-loop study that assessed TEMO operations in a flight simulator. Three Human-Machine Interfaces (HMIs) were designed in an attempt to achieve efficient pilot-automation interaction. The three HMIs differed in the level of information displayed. For comparison, data from computer simulations that used a zero-delay pilot response model,

the ‘Autobot’ runs, were used. This allowed us to investigate to which level the variations in pilot response affect the accuracy of TEMO descents. In the research presented here, we consider a scenario where flap selections and gear deployment are performed by the pilot, and TEMO automation controls the auto-throttle and auto-speedbrake. We will investigate what and how much information should be presented to support pilots operating TEMO, to maintain high levels of performance. The paper discusses the results of a pilot-in-the-loop study that assessed TEMO operations in a flight simulator. Three HMIs were designed in an attempt to achieve efficient pilot-automation interaction. The three HMIs differed in the level of information displayed. For comparison, data from computer simulations that used a zero-delay pilot response model, the ‘Autobot’ runs, were used. This allowed us to investigate to which level the variations in pilot response affect the accuracy of TEMO descents. Several metrics, such as mental workload, action delays and achieved time deviation(s) were used to assess performance of the different HMI options.

The paper is structured as follows: Section II briefly discusses the Time and Energy Managed Operations (TEMO) concept, algorithms and procedure. The role of the pilot in performing TEMO descents, and the HMIs designed to support that role are discussed in Section III. The pilot-in-the-loop experiment is described in Section IV; Section V discusses the experiment results including objective flight performance metrics and pilot responses to questionnaires. The paper ends with a discussion and recommendations, Section VI and conclusions, Section VII.

II. Time and Energy Managed Operations

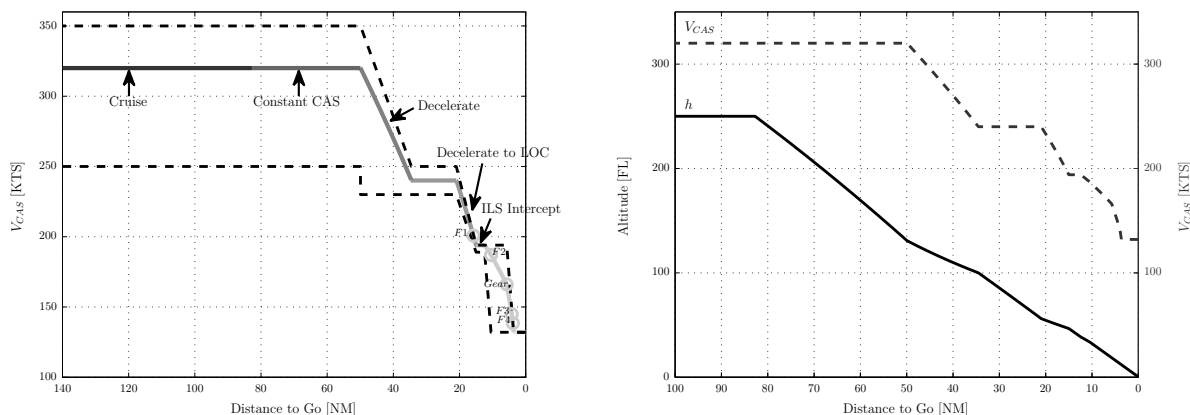
TEMO is a new CDO concept that aims at reducing fuel use, gaseous and noise emissions whilst conforming to time constraints imposed by Air Traffic Control (ATC). This section briefly describes the TEMO concept, algorithms and procedure; for a detailed discussion the reader is referred to Ref. [5].

II.A. The TEMO Concept

TEMO enhances the current aircraft vertical guidance through an optimization algorithm that calculates *energy-neutral* trajectories and employs an improved guidance function to fly these trajectories. This energy profile is calculated using true airspeed and barometric altitude. An energy-neutral trajectory requires only engine idle thrust and uses no additional drag devices during descent from Top of Descent (ToD) to the stabilization point at 1,000 ft above ground level. At the stabilization point the aircraft is stabilized, configured and ready for landing, following a conventional Instrument Landing System (ILS) procedure for this last part of the descent. To improve predictability, trajectories calculated by TEMO adhere

to the definition of a *closed-path* trajectory as defined by ICAO.⁴

The TEMO concept uses the principle of energy exchange¹³ to control the aircraft to a given point in space and time. By following a nominal calibrated airspeed profile, see Fig. 1, aircraft comply with applicable speed constraints. To arrive earlier or later, the TEMO algorithm can deviate from the nominal profile but only within prescribed speed margins. The speed profile is flown by the guidance system using Speed-on-Elevator (SOE) control of the calibrated airspeed and with thrust set to idle. This implies that the aircraft does not follow a fixed vertical profile; the actual flown vertical profile depends on aircraft characteristics and disturbances.



(a) TEMO characteristic phases (excluding Mach descent) from Top of Descent at FL 250 to the runway threshold (0 NM).

(b) Nominal TEMO altitude profile and calibrated airspeed profile (CAS vs. Distance to Go).

Figure 1. Nominal TEMO calibrated airspeed profiles and altitude profile.

Disturbances, modeling and estimation errors, can lead to a deviation from the planned trajectory in terms of time and energy (altitude and velocity).⁵ These deviations could be corrected instantaneously, using control-laws, resulting in *tactical replanning*. Another method is a *strategic replanning* approach that permits small deviations from the planned trajectory but calculates a new trajectory when these deviations exceed a predefined boundary, Ref. [5]. This relaxed method allows a deviation to evolve which could potentially result in the error resolving or changing sign. This is different from tactical replanning which would automatically react to resolve the deviation which could be sub-optimal or result in energy problems later on, however time deviations would be kept at a minimum. In the experiment discussed here, TEMO used only strategic replanning to correct deviations to provide a more relaxed corrective action.

The TEMO algorithm aims at finding an energy-neutral trajectory using *energy management*. Proper energy management allows an aircraft to exchange kinetic and potential energy, resulting in an energy-neutral trajectory, which implies that no additional energy

is added or dissipated. However, situations could occur where the TEMO algorithm cannot find a trajectory without using thrust or drag devices. In these cases, the algorithm minimizes thrust and drag device use, resulting in an *energy-optimal* trajectory. In extreme cases, the TEMO algorithm cannot find a valid trajectory that satisfies all constraints, which is referred to as a *reject*. In this case, pilots should notify ATC to negotiate new constraints or revert to a vector-based arrival.

TEMO uses time constraints for its 4D flight trajectories. A time constraint can be an absolute time constraint, using a Controlled-Time of Arrival (CTA), at a location along the trajectory,²¹ or a relative time interval to a leading aircraft using airborne spacing.²¹ The time constraints commanded by ATC include a Required Time Performance (RTP) that prescribes the required accuracy to meet time constraints for 95% of all operations. During hours of low-demand, the RTP could be set less restrictive to achieve more environmental benefits, whereas during hours of high-demand, the RTP can be set to a low value to ensure a high inter-aircraft spacing accuracy to satisfy runway throughput requirements. The current experiment used CTAs at the IAF and runway threshold for time management.

To reduce uncertainty caused by variations in pilot response during execution of the idle descent, the descent is flown using the autopilot and the aircraft cockpit displays are enhanced to support pilots in performing configuration changes during TEMO descents. The TEMO flight procedures are discussed in the next subsection.

The TEMO concept is developed and tested for the Airbus A320 aircraft; it can be adapted to allow CDOs with other modern, commercial aircraft in the future.

II.B. TEMO Flight Procedure

All required pilot actions during the TEMO procedure are illustrated in Fig. 2. During cruise, pilots receive a descent clearance that includes a CTA for the IAF from ATC through data-link. Pilots review the clearance and activate the clearance information $\textcircled{\text{CI}}$, such as Standard Arrival Route (STAR), runway, descent altitude, CTA and RTP into the FMS through Control and Display Unit (CDU) and Flight Control Unit (FCU). The CTA is then used by the FMS as a Required Time of Arrival (RTA).

Using the entered clearance details, the TEMO algorithm calculates an optimized descent trajectory that complies with the received clearance. When that is completed, pilots accept the clearance and notify ATC using data-link. Next, pilots prepare the autopilot and FMS to fly the calculated trajectory and perform the descent checklist.

At ToD, the aircraft automatically intercepts the descent trajectory, while pilots monitor flight progress. By monitoring differences between commanded speed and actual speed, possible time deviations can be anticipated.

Prior to Terminal Maneuvering Area (TMA) entry, ATC sends an updated clearance to

descend to the runway with associated CTA and RTP at the runway. Pilots again insert the clearance details $\textcircled{C2}$ into the FMS, which automatically removes the RTA information from the IAF and adjust the FCU altitude window accordingly. When the RTA_{RWY} is different from the current Estimated-Time of Arrival $(\text{ETA})_{RWY}$, the TEMO algorithm calculates a new trajectory to arrive on time.

Within the TMA, pilots perform approach and landing checklists and execute configuration changes at planned locations as demanded by the trajectory. Delays in selection of configurations could result in deviations from the planned trajectory and consequently pilots are expected to set the configurations accurately and timely.

In general, Flaps 1 $\textcircled{F1}$ is set prior to intercepting the localizer \textcircled{LOC} , followed by Flaps 2 $\textcircled{F2}$ after which the glideslope $\textcircled{G/S}$ is intercepted. Hereafter, pilots lower the landing gear \textcircled{G} to increase deceleration and set the go-around altitude. Finally, Flaps 4 $\textcircled{F4}$ is selected^a prior to reaching Final Approach Speed (FAS).

Upon glideslope intercept TEMO is automatically disengaged and no longer calculates new trajectories to correct deviations. From this point onwards, the descent is an open-loop system and hence accurate selection of configuration changes is required to limit deviations from the planned trajectory.

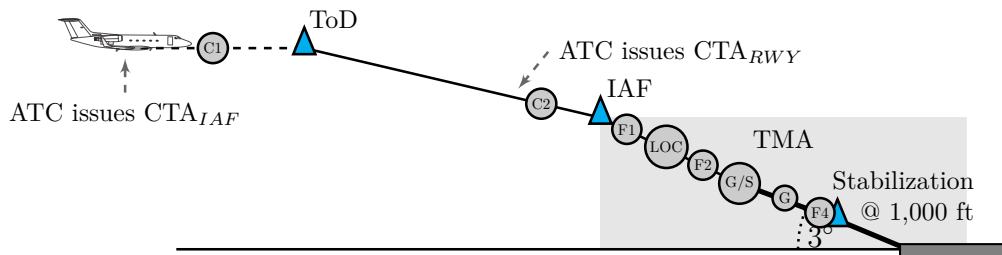


Figure 2. Overview of pilot actions during a TEMO descent.

II.C. TEMO Algorithm and Trajectory Predictor

In a preceding batch study⁵ that investigated TEMO performance, a MATLAB implementation of the TEMO algorithm was used which required at least 30 seconds to calculate a new trajectory. In the current real-time, pilot-in-the-loop experiment, a faster calculation routine was required that could be integrated into existing simulation software. Therefore, a new algorithm was developed²² in C++ using the open-source tool PSOPT.²³ PSOPT is a state-of-the-art, open-source tool that uses direct collocation methods, such as local and pseudospectral discretizations to rapidly solve optimal control problems. Using discretization techniques, continuous time can be transformed into a number of finite nodes, which reduces

^aTo reduce the number of pilot actions, the HMI commands pilots to select Flaps 4 at the location of Flaps 3 since Flaps 4 succeeds Flaps 3 almost instantly at that particular deceleration rate.

the optimal control problem from an infinite dimensional problem into a finite, non-linear programming problem. The TEMO implementation used in this experiment used PSOPT based on IPOPT²⁴ and uses the ADOL-C²⁵ automatic differentiation package to generate first and second order derivatives.

In this experiment, it is assumed that geometric and barometric altitude are equal as there are no differences in pressure fronts simulated in this experience. As such, energy is calculated using the true airspeed and geometric altitude.

Besides simplified aircraft modeling to improve calculation time, the glideslope is not included in the optimization algorithm for the same reason. Consequently, the algorithm only optimizes the trajectory from ToD (or current position) down to the glideslope intercept point. As a result, the deviation boundaries are deactivated upon intercepting the glideslope and any disturbance that occurs while descending down the glideslope will not be corrected for, nor can the TEMO algorithm command additional thrust or speedbrakes while the aircraft descends down the glideslope.

Table 1. TEMO deviation thresholds and Required Time Performance (RTP).

Active CTA	RTP [s]	Deviation Boundary					
		Top of Descent		IAF		Runway Threshold	
		<i>Time [s]</i>	<i>Energy [ft]</i>	<i>Time [s]</i>	<i>Energy [ft]</i>	<i>Time [s]</i>	<i>Energy [ft]</i>
IAF	5	±10	±400	±5	±200	-	-
Runway	2	-	-	±4	±200	±2	±100

The algorithm calculates earliest and latest achievable ETAs at the time-constrained waypoint to inform pilots of the achievable time window. These ETAs are broadcast to ATC through data-link to provide ATC with information for sequencing and spacing of aircraft.

Once a deviation exceeds a boundary and remains out of bounds for 10 seconds, the algorithm calculates a new, optimized plan that returns the aircraft to the center of the boundaries upon automatic plan activation. The boundaries (Table 1) are defined as a positive and negative value; these values become smaller while approaching the time-constrained waypoint, as the ‘control space’ decreases. Note that the RTP values are smaller than the prescribed 10 seconds accuracy used in the Initial 4D project²⁶ of SESAR, in an attempt to further increase capacity.

Replanning is disabled when the aircraft is too close to a time-constrained waypoint, or too close to the glideslope intercept, as both the calculation process requires time and the available distance to correct for a deviation is limited. Before replanning, a position and altitude constraint is *predicted* serving as initial position for replanning. This constraint is located 20 seconds in front of the current position along the active plan. However, a replan must be calculated within 18 seconds to provide a 2 second window to transition to the new trajectory. If the replan was not successful within 18 seconds, the FMS reports a reject.

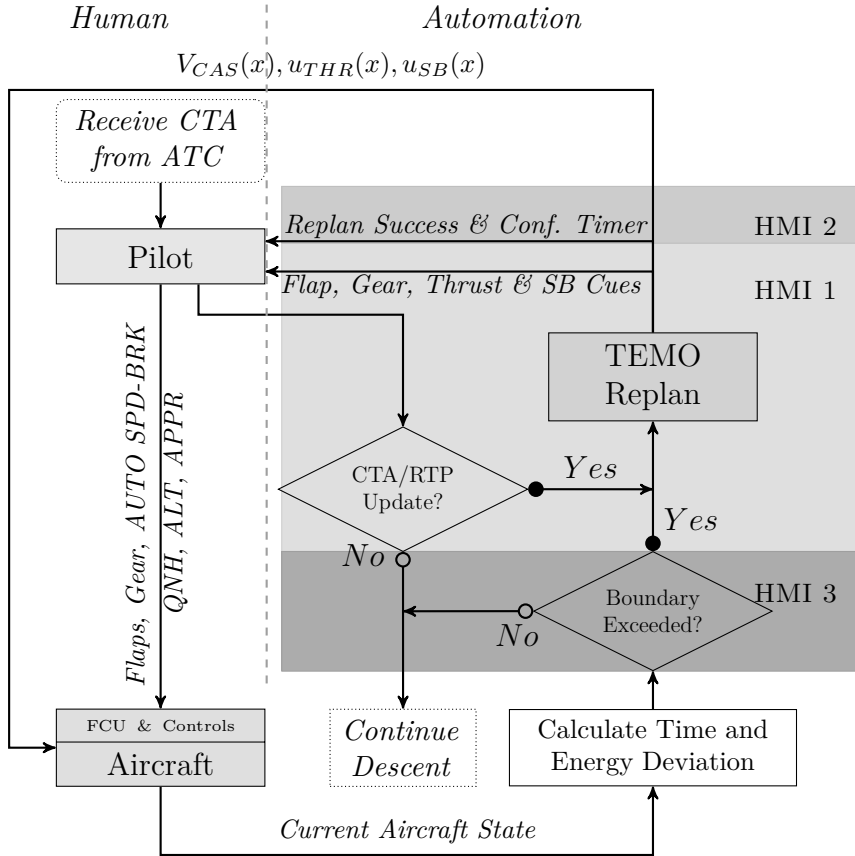


Figure 3. Schematic of the pilots' role in TEMO and the information displayed by the HMI variants.

III. TEMO Human-Machine Interface Designs

In this paper we investigate how much and what information is required to perform TEMO descents using strategic replanning. Three HMI variants were designed (Fig. 5), that differ in the amount of information presented. All displays allow efficient human-machine interaction and aimed at minimizing variations in the pilots' response. The TEMO-specific elements were designed using a constraint-based approach,^{27,28} inspired by Ecological Interface Design (EID),¹⁹ to provide more transparency by visualizing the automation constraints required by the TEMO algorithm to calculate a new trajectory through strategic replanning.

The role of the pilot in the TEMO concept is illustrated in Fig. 3. The figure also shows the different elements added to the cockpit displays in support of TEMO to each of the three HMI variants.

Each subsequent HMI variant contains the elements of its predecessor, and has new functions (more information) displayed. Besides these specific features, the RTA page of each waypoint on the CDU has been adapted to present earliest and latest achievable ETAs and RTP information. All elements were designed for the Airbus A320 cockpit, a typical modern aircraft.

III.A. HMI Variant 1

The baseline HMI variant includes only new elements that are required for TEMO operations. The new features added to the displays are listed below.

AUTO-SPEEDBRAKES TEMO uses a novel flight control system referred to as auto-speedbrakes, inspired by Airbus' A318 steep-approach²⁹ system to perform steep ILS approaches into London City Airport. Boeing also developed an auto-drag function³⁰ for the Boeing 787 that controls speedbrakes to increase the aircraft descent rate when above path. This system is especially useful when intercepting the ILS glideslope from above.

The TEMO auto-speedbrakes function controls speedbrakes as demanded by a planned trajectory to reduce pilot workload. Pilots operate the system by enabling the auto-speedbrake function on the overhead panel and by setting the speedbrake lever. The lever position limits the maximum deflection allowed by the planning and guidance functions, similar to the use of auto-thrust on Airbus aircraft.

FLAP AND GEAR CUES The TEMO algorithm plans the position where configurations must be set, based upon a fixed calibrated airspeed that depends on the minimum maneuvering speed.⁵ The configuration change speed is shown on the the Primary Flight Display (PFD) speed tape and a flap 'hook', left of the speed-tape, shows the second next flap speed.

The speed tape also shows the commanded Calibrated Airspeed (CAS), commanded speed-trend (extended from the bullet) and speed target (magenta triangle). If the commanded speed and target speed are equal, the speed will remain constant until a change in flight-path angle as drawn on the Vertical Situation Display (VSD).

The predicted locations where configuration speeds are obtained are visualized on the Navigation Display (ND) and VSD as a pseudo-waypoint to improve observability. These pseudo-waypoints are the primary cue for selecting configurations as this provides a self-correcting mechanism for deviations. Although TEMO commands a speed profile, small time deviations could still occur. For example, when the aircraft is ahead of schedule the configuration change location is reached earlier, such that a selected configuration generates additional drag. To avoid decelerating below the minimum maneuvering speed an offset of 5 KTS is added to obtain the configuration speeds.

THRUST AND SPEEDBRAKE CUES Use of thrust and speedbrakes are in principle undesired since these actions are not energy-neutral and sub-optimal in terms of environmental impact; they may also cause engine spooling and vibrations due to aerodynamic drag. To inform the pilots, the planned locations of additional thrust or speedbrake use in excess of 5% and 2.5%, respectively, are drawn on the ND and VSD.

III.B. HMI Variant 2

To improve situation awareness, a configuration timer and notifications of successful replans were added to the baseline, yielding HMI variant 2.

CONFIGURATION TIMER To support pilots in selecting the next configuration, a timer is added to the right of the PFD speed-tape as shown in Fig. 5. The timer is visible 20 seconds prior to reaching the predicted location of the configuration change and starts to count down 10 seconds later. Once the timer is visible, disturbances occurring between this point and the actual configuration change do not change the countdown time or countdown speed. Any speed deviations during this time window could therefore cause the timer to finish too early or late.

REPLAN NOTIFICATIONS In all HMI variants, the display informs pilots of an active replan calculation by removing all FMS predicted values from the CDU, ND and VSD. Hence, all fuel and time predictions are displayed as dashes when the system is replanning. To improve directability, the TEMO algorithm informs pilots of a rejected replan through messages on the Flight Mode Annunciator (FMA) and CDU. In this case, the aircraft remains flying the old plan until pilots select a different flight mode, or remove constraints to activate a new replan. Optionally, when a replan was successful, a message shows **PLAN CHANGE** on the ND in variants 2 and 3.

III.C. HMI Variant 3

HMI variant 3 presents a Time and Energy Indicator (TEI) to increase pilot awareness of sustained deviations.

TIME AND ENERGY INDICATOR Time and energy deviations are shown on the TEI, illustrated in Fig. 4. Current thresholds are given by the current aircraft position and values of Table 1; these thresholds reduce during the descent (③). The TEI follows an ‘inside-out’ reference, as the position of the magenta marker represents the *planned* aircraft time and energy states (②), while the cross marking the center (①) indicates the *actual* states; the situation depicted in Fig. 4 shows an aircraft being late (i.e., behind schedule) and low on energy. The boundaries (③) change color when the planned indicator exceeds a boundary and a replan will commence when the indicator remains 10 seconds outside the boundaries.

The TEI provides an indication of possible replan solutions, as a low energy state or expected late arrival can be resolved using thrust, while speedbrakes can be assigned to a high energy state or too early arrival (light-gray areas). When the aircraft is rather early and low on energy, correct energy exchange could resolve the deviation (white areas). Since

an aircraft flying fast and low could have an equal level of total energy as an aircraft flying slow and high, pilots should monitor speed and altitude indicators to deduce the cause of energy deviations. Hence, the TEI is primarily designed to anticipate replans and improve TEMO's observability and directability.²⁰

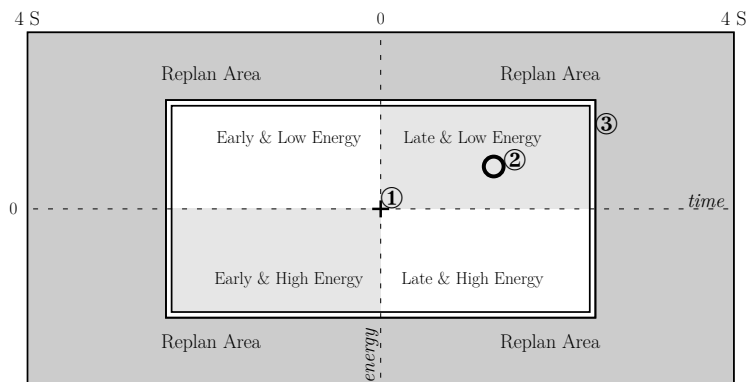


Figure 4. Working principle of the Time and Energy Indicator (TEI): (1) Current Time and Energy position; (2) Planned Time and Energy position; (3) Current Time and Energy boundaries.

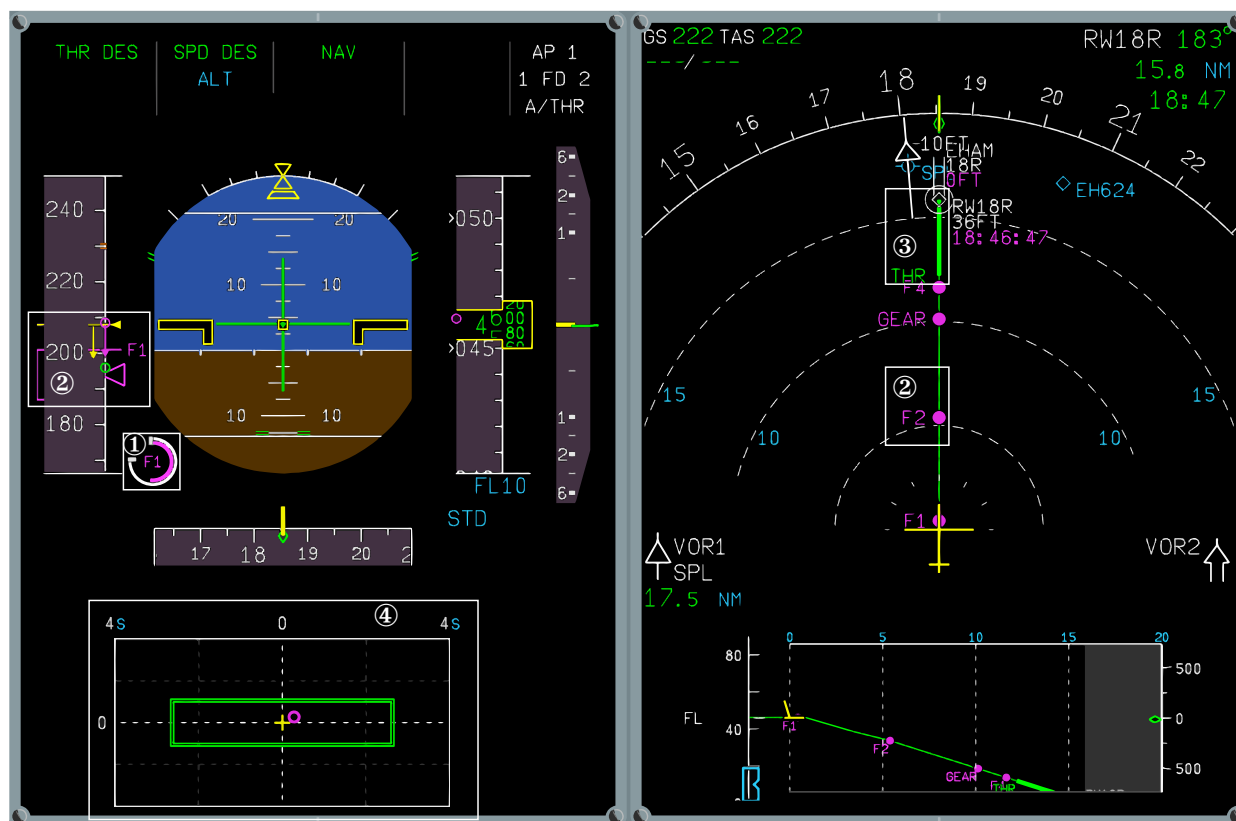


Figure 5. Overview of the three HMI variants with TEMO functions: (1) Configuration Timer; (2) Configuration Cues and Commanded Speed; (3) Additional Thrust (THR) Cue; (4) Time and Energy Indicator.

The resulting three HMI variants are shown in Fig. 5, with the four main TEMO functions indicated with the numbered white circles 1–4. Here, the TEI (bottom left) indicates that the aircraft is only slightly late and a little low in energy.

IV. Experimental Evaluation

This experiment evaluates the human role in the TEMO descent procedure and aims to compare the three HMI variants. Experimental variations were limited to controlled disturbances such that all observed deviations were caused by expected variations in pilot response. Metrics evaluated included mental workload and TEMO performance expressed as time deviation from the CTA at the runway threshold.

The primary objective of the experiment was to receive feedback regarding the HMI variants and TEMO procedures. Results were evaluated in qualitative fashion; whenever appropriate statistical tests were conducted to study the significance of the results. Besides the runs flown with actual pilots, several scenarios have also been flown using an automated, zero-delay pilot response model, referred to as the ‘Autobot’. Comparing the piloted runs with the Autobot runs will shed a light on whether the HMI variants have successfully mitigated the variations in pilot response.

IV.A. Method

IV.A.1. Pilot Subjects

Nine professional airline pilots, Table 2, participated in the experiment as Pilot Flying (PF). Their total flight hours ranged between 1,050 hours and 18,200 hours ($\bar{X} = 8,200$ hours, $\sigma_X = 5,988$ hours); their age ranged between 32 and 78 years ($\bar{X} = 50.33$, $\sigma_X = 13.63$). Five pilots had previous data-link experience, two pilots had experience with using a VSD, six pilots had experience with CTAs, and seven pilots had experience with flying Continuous Descent Approaches (CDAs).

Pilots received an extensive briefing guide, informing them about the TEMO concept, the novel display elements and experiment set-up. They were instructed to adhere to Standard Operating Procedure (SOP) and the newly defined TEMO procedure introduced in Section II.B as much as possible. In addition, pilots were told to adhere to these procedures also in cases where they expected *not* to meet the CTA or reach the stabilization requirements before passing 1,000 ft.

The subject pilots acted as PF and were accompanied by a host-pilot^b as Pilot Not Flying (PNF).

^bAll host-pilots are, or were, licensed test pilots and also supported the TEMO developers during set-up of the experiment and design of the new cockpit-displays.

Table 2. Characteristics of pilot participants in the experiment.

Pilot	Age	Flight Hours	CDA Experience	Aircraft Types
1	51	13,820	yes	B737, B747, B777, MD-11, C500
2	36	2,700	yes	Cessna Citation C550, PA31, DA42, BE18
3	58	14,000	yes	DC-9/10, A310-200, MD-11, B747, A320, B737
4	32	4,000	yes	B737, A319
5	47	6,630	yes	MD-11, B747, A330
6	78	9,500	no	Fokker 27, Fokker 50, Fokker 28, Fokker 70/100, F104, F16
7	54	3,900	no	Fokker 70/100, various Cessna and Gulfstream business jets
8	42	1,050	yes	Cessna Citation 550, Fairchild Metroliner II
9	53	18,200	yes	Fokker 27, B747, A310, MD-11, B777

IV.A.2. Apparatus

The experiment was performed at NLR’s Avionics Prototyping Environment for Research and Operations (APER0), a fixed-base research flight simulator providing flexible avionics prototyping. APER0 has a modular cockpit and comprises five high-resolution touchscreen LCDs that simulate cockpit displays. A High Definition LCD-TV displays the outside visual using Microsoft Flight Simulator X.

Pilots controlled the aircraft using the FCU and CDU, by setting the correct FCU altitude, lateral and vertical autopilot modes. Although manual flying was possible, pilots were instructed to fly the aircraft using the autopilot. The CDU was used to enter and review CTA information and trajectory data; the Data Communications Display Unit (DCDU) was used to send and receive data-link messages.

IV.A.3. Independent Variables

Two independent variables were manipulated. First, the three *HMI variants* of Section III were simulated, which vary in the amount of additional information presented. The small differences between the HMI variants should allow for an investigation of the individual display items that were added or removed from each subsequent variant.

The second independent variable was an *error disturbance*, which consisted of four levels. The first level contained *no disturbance* throughout the entire descent and was used as a baseline.

The second disturbance level was an *energy error*, introduced by commanding the autopilot to intercept the descent 10 seconds early, resulting in a continuously growing altitude deviation and, consequently, in a total energy deviation (as both potential as well as kinetic energy are affected) with respect to the planned trajectory.

The third disturbance level introduced an *offset time constraint* at the runway. By issuing a CTA_{RWY} at the runway threshold that significantly differs from the current ETA_{RWY} at the threshold, an instantaneous time deviation occurs, exceeding the current time boundary to force a replan. Depending on the size of this time deviation, an energy-neutral or energy-

optimal plan is found by the TEMO algorithm. The commanded CTA_{RWY} value was such that a replan would result in an energy-optimal plan requiring thrust and/or speedbrakes.

The fourth disturbance level introduced *both* a growing energy error and an instantaneous time error. Fig. 6 shows a schematic overview of a typical experiment scenario and the location of disturbances shown using dashed arrows.

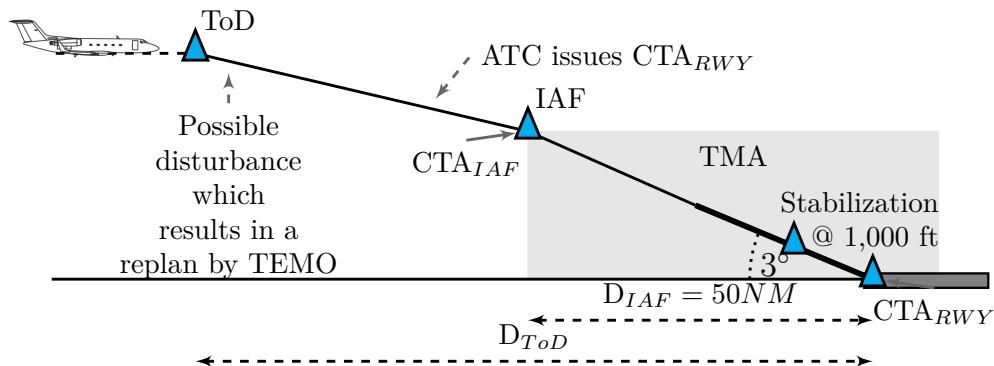


Figure 6. Overview of a typical TEMO experimental scenario.

IV.A.4. Scenarios

The measurement runs consisted of twelve scenarios, see Table 3. The first half was designed as a within-subjects repeated-measures design, defining six scenarios consisting of the three HMI variants and the first two disturbances. This allows for a full comparison between the three HMI variants for these disturbances and a comparison between disturbances for each HMI variant.

The second half of the scenarios contained the third and fourth disturbances. The CTAs differed per scenario so pilots would experience both earlier and later arrivals. For the same reason, the energy disturbance, a combination of a time and energy error, is also different.

For a full factorial design, two additional levels in the disturbance variable should have been introduced, resulting in six additional runs and approximately three hours of additional simulation time. With a total experiment time of one and a half day per pilot, it was decided not to fully include these conditions and hence combine the earlier and later arrivals into a single variable level. As a consequence, these scenarios were not used in statistical analyses.

The objective of the experiment was to test nominal TEMO operations and procedures using absolute time management; therefore, no other traffic or emergency situations (such as engine failures) were modeled that could disrupt TEMO operations.

The twelve scenarios are depicted in the experiment matrix shown in Table 3. This matrix also shows the scenario number and type and/or amount of disturbance introduced in that scenario. The second number in the scenario number reflects the disturbance variable while the last number reflects the HMI variant. Scenarios 111–123 have been used in the

statistical analysis discussed in the next section.

Table 3. Experiment Matrix of the pilot-in-the-loop experiment.

	Scenario											
	111	112	113	121	122	123	131	132	133	141	142	143
HMI Variant	1	2	3	1	2	3	1	2	3	1	2	3
Disturbance												
<i>CTA Offset [s]</i>	0	0	0	0	0	0	+25	-20	+25	-35	+15	-35
<i>Energy Error</i>	-	-	-	ToD	ToD	ToD	-	-	-	ToD	ToD	ToD

All pilots flew the scenarios in a randomized order to counteract learning effects using a mixed random-balanced Latin Square design. As only nine pilots could participate in the experiment, a full Latin Square design was not possible. Therefore, nine rows out of a 12×12 Latin Square were randomly assigned to each of the nine pilots.

IV.A.5. Approach Conditions and Aircraft Characteristics

Each scenario started at FL 250 in cruise phase and 18 NM from ToD and located 120 NM from Amsterdam Airport Schiphol runway 18R. The aircraft was trimmed at 320 KIAS, in clean flaps configuration with the landing gear retracted and at 90% Maximum Landing Weight (MLW). The trajectory was a straight-in descent and pre-programmed in the FMS. The lateral trajectory was fixed and the IAF was located 50 NM from the runway threshold. The vertical profile was optimized by the TEMO algorithm up to glideslope intercept and continued as a 3° path to the runway.

The simulation used a high-fidelity, non-linear aircraft model of the Airbus A320.³¹ From this model, a simplified point-mass model was derived for use by the TEMO algorithm. The autopilot included modes for lateral and vertical navigation (Lateral Navigation (LNAV)/Vertical Navigation (VNAV)), localizer and glideslope intercept and used a non-moving auto-thrust system.

The atmosphere was modeled using the International Standard Atmosphere (ISA); neither wind nor turbulence were simulated, to reduce variations.

IV.A.6. Procedure

The experiment began with training runs and continued with measurement runs. The training started with a briefing and a Q & A session, and continued in the APERO simulator to introduce the three HMI variants. The training runs allowed pilots to familiarize with aircraft controls and dynamics, and the operation of Controller Pilot Data Link Communications (CPDLC) and new FMS functions.

In total, the experiment required one and a half day per pilot to fly all training and measurement runs. A single simulation scenario required approximately 25 minutes to complete.

After every simulation, pilots were asked to fill out a post-run questionnaire, with questions about the flown simulation. Pilots indicated their Rating Scale Mental Effort (RSME)³² on a single analog scale, which makes it easier and simpler to use than for instance NASA-TLX which uses multiple scales.³³ In addition, pilots rated their trust in the automated system using a modified version of the Controller Acceptance Rating Scale (CARS)³⁴ rating scale, developed for automated systems in ATC. Open-ended questions, related to the TEMO concept and procedures, served as explanatory answers to the rating scales. The questionnaire concluded with three open-ended questions, which asked pilots whether they met the time-constraints within the allowed RTP at TMA entry and runway threshold, and whether the final approach was stabilized at 1,000 ft.

At the end of the experiment, pilots filled out the final post-experiment questionnaire about the TEMO concept. Pilots indicated their agreement with statements concerning safety, acceptance, thrust and speedbrake use, situational awareness, configuration changes on a 5-point Likert scale ranging from strongly disagree to strongly agree. Moreover, pilots were asked to rate their preference about the HMI variants and TEMO features.

IV.A.7. Dependent Measures

Dependent measures were grouped into objective and subjective measures. Objective measures were:

Pilot Performance Pilot performance was measured by calculating the delay in selecting configurations. Any delay, either negative or positive, from the planned position will result in a deviation from the planned trajectory, which could lead to time and/or energy deviations. The time deviation could eventually result in a time offset at the threshold that exceeds the RTP. The deviation from the assigned CTA_{RWY} at the runway threshold and the time deviation at the IAF were also determined to establish how well the time goals were met. These time deviations for pilot runs are compared with the results from Autobot to analyze effects of pilot response.

Environmental Impact Environmental impact was compared between the piloted runs and the Autobot runs, to investigate the effects of pilot variations. The noise impact of each run is evaluated using the total area of the 75 dB Sound Exposure Level (SEL) noise contour. A noise model, based on the ECAC/CEAC Document 29 specification³⁵ is used to calculate the 75 dB SEL contour. Moreover, the amount of Nitrogen Oxide (NO_x) emissions below the mixing height of 3,000 ft is calculated using the Boeing Method 2³⁶ model. Finally, the amount of fuel burned is analyzed.

By filling out the post-run and post-experiment questionnaires, pilots were asked to provide their subjective assessments regarding workload, TEMO procedures and system, safety

and perception of their performance. Subjective measures obtained from these questionnaires were:

Workload Pilots were asked to rate their RSME per scenario as a metric for workload.

The absolute scores provided by the pilots are subjective and one pilot might rate all scenarios relatively high on the RSME scale whereas another pilot might rate all approaches low on the RSME scale. Since we are only interested in relative performance per display and per disturbance, the RSME scores are transformed into z -scores³⁷ per pilot to remove this variability.

TEMO In the post-experiment questionnaire, pilots were asked to express their preference for one of the three HMI variants and the specific TEMO display details in terms of usefulness and representation. These answers were used to understand their preference for a particular HMI variant and are, as such, not a metric itself.

Safety The stabilization criteria have been objectively set to the criteria listed below. At 1,000 ft, the aircraft should be: *a) FAS $\leq V_{IAS} \leq$ FAS+20; b) flaps are set for landing; c) landing gear is down; d) thrust is stabilized to maintain Final Approach Speed; e) less than 1 dot deviation from the localizer and glideslope; f) all checklists and briefings are completed.*

After each simulation, pilots were asked to rate on a 5-point Likert scale their judgment regarding the safety of the flown approach. Additionally, pilots were asked whether they thought to have been stabilized when descending through 1,000 ft, which was verified with objective results.

IV.B. Experimental Hypotheses

Based on the experiment objectives, the following hypotheses were formulated:

Hypothesis 1. *Pilots will be able to meet assigned time and stabilization requirements with all HMI variants. This makes HMI variant 1 the required variant and HMI variant 2 the preferred variant.*

Hypothesis 2. *Although HMI variant 1 provides the necessary information, it is expected that pilot will prefer the additional information provided by variant 2, but that the most extensive variant 3 will be found too cluttered.*

Hypothesis 3. *Pilots accept the arrivals that are flown and find the TEMO procedures acceptable.*

Hypothesis 4. *There will be no significant influence of pilot timing on the TEMO performance, and thus it is expected that there will be no substantial difference in environmental impact between the Autobot and piloted runs.*

V. Results

The experimental results will be discussed, starting with TEMO performance in terms of time deviations and pilot acceptance, followed by evaluating pilot subjective responses to the questionnaire. In addition, the time performance and environmental impact between all scenarios flown with pilots and scenarios flown with the Autobot will be compared.

V.A. TEMO Performance

V.A.1. Time of Arrival Performance

Fig. 7(a) shows the time deviation when the aircraft passes the IAF for scenarios including the two disturbances (no disturbance, energy disturbance at ToD) under consideration for each HMI variant. The HMI shows no effect on the time deviation at this location, which could be expected as up to the IAF the influence of the pilot (and hence, the display) is limited: no configurations have to be selected prior to passing the IAF. The only ‘variation’ up to this point is how quickly the pilot enters the received CTA_{RWY} data into the CDU, which determines the initial position of a replan. Hence, this ‘disturbance’ has no significant effect on the time deviation at the IAF.

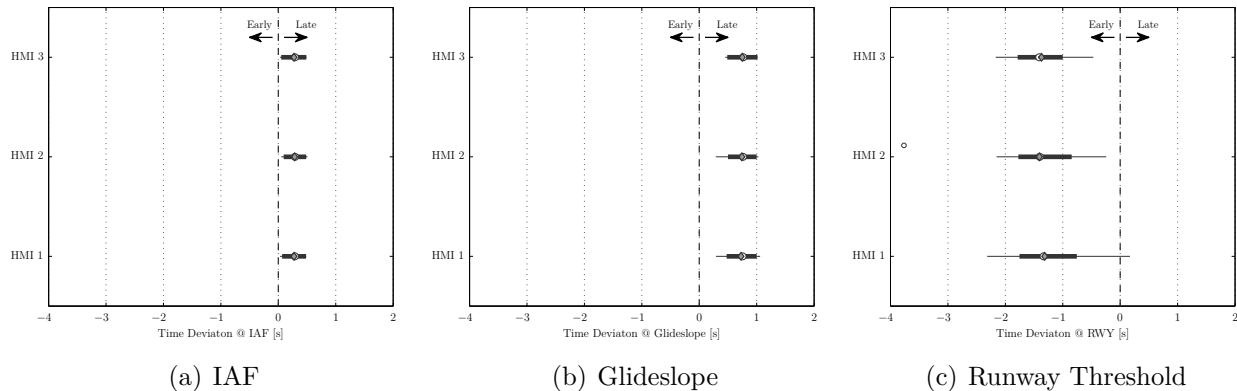


Figure 7. Time Deviation at the IAF, glideslope and runway threshold for each HMI variant ($N = 18$).

At the glideslope intercept, the TEMO replanning is disabled. Here the time deviation has grown slightly, see Fig. 7(b), but remained within a 1 second accuracy. Interestingly, the time deviation at the runway threshold, see Fig. 7(c), shows a bias to arrive *early* with respect to the assigned CTA_{RWY} and the time deviation has shifted sign and increased in magnitude. These results show that the aircraft gained approximately 1.9 seconds between glideslope intercept and the runway. Analysis showed that the aircraft typically had excess energy upon glideslope intercept ($\tau = -0.747, p < 0.001$, Kendall’s tau two-tailed). This difference in energy deviation resulted from smaller deviations between planned and actual flown trajectory. As a result of this energy deviation, the initial part of the glideslope is

flown with a higher airspeed leading to earlier arrival.

Twelve of the 108 simulation runs flown with pilots did not meet the required RTP at the runway threshold of ± 2 seconds ($\bar{X} = 1.246$ seconds *early*, $\sigma_X = 0.668$ seconds, $N = 108$). The earliest arrival was 3.766 seconds early while the latest arrival was 0.367 seconds late. In all cases of RTP violations, the aircraft was planned to arrive on time when TEMO replanning was disabled; deviations while on the glideslope were not corrected.

The time deviation at the runway, $t_{e_{RWY}}$, Fig. 7(c), deviated from a normal distribution due to a single outlier in scenario 112 ($D(9) = 0.297, p = 0.021$). Since the Analysis of Variance (ANOVA) test is relatively robust to non-normality when sample sizes are equal,³⁷ a two-way, repeated-measures ANOVA was performed on the time deviation at the runway. Due to the small sample size, the statistical analysis should be considered merely as an indication of possible effects, however. ANOVA results are summarized in Table 4.

Mauchly's test showed that sphericity was not violated for the display variable, while sphericity need not to be considered for the disturbance variable, as it only had two degrees of freedom. For the three HMI variants, the time deviations are very similar, see Fig. 7(c), confirmed by the results of the two-way ANOVA.

For validation, a two-way Friedman test that adjusts for possible row effects³⁸ but does not test interaction effects, was performed to verify the assumption of ANOVA's robustness. The results indicate that there was indeed no significant effect ($\chi_F^2(2) = 0.408, p = 0.816$) for the HMI variable.

The ANOVA results show a significant main effect caused by the disturbance variable; the disturbance triggers a replan after ToD. This updated trajectory extended the flight duration, as the time constraint at the runway is inactive and leads to a significantly reduced energy deviation, $E_{e_{GS}}$, at the glideslope intercept point. The energy deviation at the glideslope, resulting from modeling errors, violated normality for scenarios 111 ($D(9) = 0.289, p = 0.029$) and 112 ($D(9) = 0.315, p = 0.011$). The smaller energy deviation reduces the amount of energy exchange during the transition towards the glideslope, resulting in reduced speed deviations and hence time deviations. ANOVA results show no significant interaction between the display and disturbance variables.

V.A.2. Configuration Delays

Pilots were instructed to perform configuration changes, see Fig. 2, when the aircraft passes a pseudo-waypoint located along the route. Since the configuration timer is not present in all HMI variants, the deviation between selection of a configuration and the moment of passing the pseudo-waypoint is used to evaluate the effect of the timer.

In the first configuration, normality ($D(9) = 0.327, p = 0.006$) was violated for Flaps 1, τ_{F1} , due to a single outlier in scenario 123 where the pilot was distracted and selected

Table 4. Results of two-way Repeated Measures ANOVA tests.

Metric	Variable	ANOVA	Significance	Mauchly's Test	Greenhouse-Geisser Correction		
t_{CRWY}	HMI	$F(2, 16) = 0.268$	$p = 0.769$	$\chi^2(2) = 5.964$	$p = 0.051$		
	Disturbance	$F(1, 8) = 59.299$	$p < 0.001^{***}$				
	Interaction	$F(2, 16) = 0.681$	$p = 0.520$	$\chi^2(2) = 0.859$	$p = 0.651$		
E_{CGS}	HMI	$F(2, 16) = 1.264$	$p = 0.309$	$\chi^2(2) = 1.850$	$p = 0.396$		
	Disturbance	$F(1, 8) = 21.062$	$p < 0.010^{**}$				
	Interaction	$F(2, 16) = 1.072$	$p = 0.366$	$\chi^2(2) = 2.250$	$p = 0.325$		
τ_{F1}	HMI	$F(2, 16) = 2.924$	$p = 0.083$	$\chi^2(2) = 3.895$	$p = 0.143$		
	Disturbance	$F(1, 8) = 2.473$	$p = 0.154$				
	Interaction	$F(2, 16) = 0.199$	$p = 0.822$	$\chi^2(2) = 9.818$	$p = 0.007^{**}$	$F(1.140, 9.122) = 0.199$	$p = 0.698$
τ_{F2}	HMI	$F(2, 16) = 6.646$	$p = 0.008^{**}$	$\chi^2(2) = 1.236$	$p = 0.539$		
	Disturbance	$F(1, 8) = 11.133$	$p = 0.010^{**}$				
	Interaction	$F(2, 16) = 2.278$	$p = 0.135$	$\chi^2(2) = 3.378$	$p = 0.185$		
τ_G	HMI	$F(2, 16) = 0.284$	$p = 0.757$	$\chi^2(2) = 6.237$	$p = 0.044^*$	$F(1.258, 10.064) = 0.284$	$p = 0.658$
	Disturbance	$F(1, 8) = 11.891$	$p = 0.009^{**}$				
	Interaction	$F(2, 16) = 1.246$	$p = 0.314$	$\chi^2(2) = 7.665$	$p = 0.022^*$	$F(1.201, 9.607) = 1.246$	$p = 0.303$
τ_{F4}	HMI	$F(2, 16) = 0.648$	$p = 0.536$	$\chi^2(2) = 9.729$	$p = 0.008^{**}$	$F(1.142, 9.138) = 0.648$	$p = 0.461$
	Disturbance	$F(1, 8) = 4.219$	$p = 0.074$				
	Interaction	$F(2, 16) = 0.940$	$p = 0.411$	$\chi^2(2) = 26.114$	$p < 0.001^{***}$	$F(1.012, 8.097) = 0.940$	$p = 0.362$

*, Significant at the 0.05 level; **, Significant at the 0.01 level; ***, Significant at the 0.001 level.

Flaps 1 rather late. Results of a two-way repeated measures ANOVA are shown in Table 4. Sphericity was not violated and the result of the ANOVA showed no significant effect for the HMI variant, disturbance or interaction between both independent variables.

The delays in selection of Flaps 2, τ_{F2} , were all normally distributed. Sphericity was valid and the resulting ANOVA showed a significant effect of the HMI variant on the selection delay. A post-hoc pairwise comparison, adjusted with a Bonferroni correction, showed that HMI variant 1 performed worse than HMI variant 2 and 3. The disturbance variable also showed a significant effect, with earlier selections for the ‘no disturbance’ scenarios and relatively later selections during ‘energy disturbance’ scenarios. Finally, the ANOVA showed no significant effect for interaction between the two variables.

The data for gear extension also followed a normal distribution. Since sphericity was violated, a Greenhouse-Geisser correction was applied. The effect of HMI variant was not significant while the effect of a disturbance was significant. No significant interaction effects were found.

The timing of the last configuration change, to Flaps 4, violated normality ($D(9) = 0.330, p = 0.005$) due to two outliers in scenario 121. In both cases, pilots were distracted and selected full flaps too late. Mauchly’s test indicated that sphericity was violated and none of the results proved significant.

Interestingly, runs with an energy disturbance at ToD also have a significantly smaller selection delay for Flaps 2 and Gear. Similar to the time deviation at the runway, this is the result of the new trajectory resulting from a replan to correct the energy disturbance. Analysis showed that differences between the actual flown trajectory and the planned trajectory, resulting from modeling errors, were smaller for these scenarios. These smaller deviations

improved the prediction of the timer start location. The selection delay of Flaps 2 and Gear was affected by the disturbance, this also suggests that pilots often relied on the timer for configuration selections.

Levene’s test of homogeneity of variance (Table 5) showed that the variance of selection delay for HMI variant 1 (without a configuration timer) is different from the other two variants. The configuration timer supports pilots in selecting flaps and gear effectively, resulting in reduced variance in the selection delay.

A non-parametric rank correlation analysis was performed between the time deviation at the runway threshold and the configuration delays, to investigate whether these delays affected time performance at the runway threshold. The results, shown in Table 6, reveal that only the timing of the last flap configuration shows some correlation with the accuracy of arrival time. The possible mechanism for this is first that the drag change and effect on flight speed due to the flap extension are considerable, and second that the algorithm at this stage no longer corrects time deviations.

V.B. Questionnaires

PILOT WORKLOAD AND TRUST Fig. 8 shows the averaged RSME ratings and z -scores for each of the three HMI variants and all scenarios. RSME serves as a measure for workload. From this figure, no differences in RSME rating between the three HMI variants can be identified. A two-way repeated measures ANOVA on the transformed RSME z -scores of scenarios (111–123) showed no significant differences for the display and disturbance variables.

Over all questionnaires, one can conclude that the average RSME remained well below 30, which corresponds to less than ‘Little Effort’.³²

Pilots rated their trust in the automated TEMO system using the CARS rating scale while considering all scenarios and the limited scope of the experiment. Their scores ranged

^bOne questionnaire was lost through the course of the experiment; all scores from this pilot were removed.

^dOne questionnaire was lost and two questionnaires did not contain RSME scores.

Table 5. Results of Levene’s test of homogeneity of variance for the configuration delays.

	Conditions Tested					
	HMI 1 & HMI 2		HMI 1 & HMI 3		HMI 2 & HMI 3	
	F	p	F	p	F	p
Flaps (1, 106)	10.028	< 0.01**	12.463	< 0.001***	0.669	0.415
Gear (1, 34)	3.665	0.064	5.181	< 0.05*	0.454	0.505
σ_{flaps}^2	7.739	1.104	7.739	0.888	1.104	0.888
σ_{gear}^2	5.918	0.961	5.918	0.486	0.961	0.486

*, Significant at the 0.05 level; **, Significant at the 0.01 level; ***, Significant at the 0.001 level.

Table 6. Kendall tau correlation for the configuration delays vs. time deviation at runway threshold.

Configuration	Correlation Coefficient	Significance
Flaps 1	$\tau = -0.010$	$p = 0.923$
Flaps 2	$\tau = 0.049$	$p = 0.607$
Gear	$\tau = 0.089$	$p = 0.347$
Flaps 4	$\tau = 0.214$	$p = 0.023^*$

*, Significant at the 0.05 level.

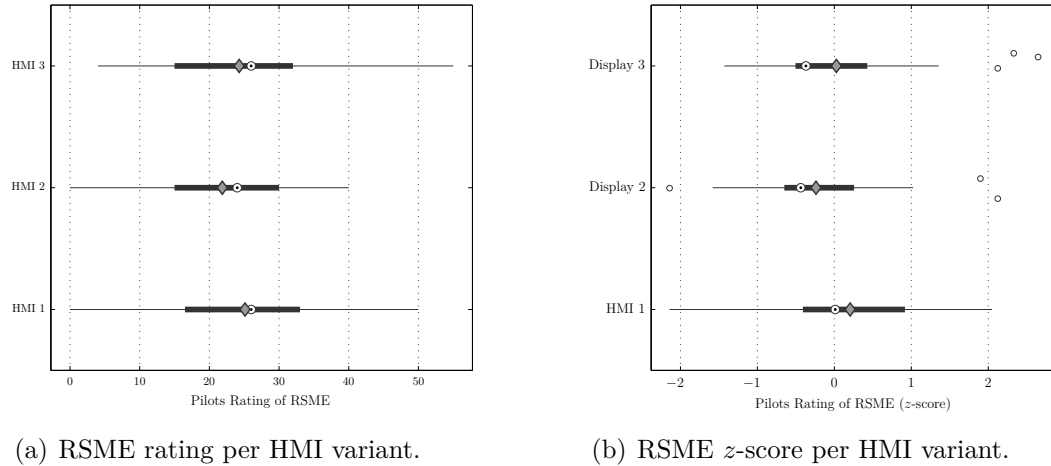


Figure 8. RSME ratings and z-scores per HMI variant ($N = 105^d$) including mean (diamond) and median (circle).

between 6 (some improvement) and 9 (quite acceptable), ($\bar{X} = 7.44, \sigma_X = 1.13$).

TEMO FEEDBACK All pilots indicated that the configuration changes were manageable and that they were “in the loop” throughout the entire experiment. Pilots indicated that the TEMO procedures were clear and acceptable. 67% of pilots found the procedures complete but some answered that procedures for CTA negotiation should be improved as communication could increase workload.

Some pilots argued that the required time accuracy at the runway threshold could be too strict in real-life operations with wind and turbulence. They argued that using fixed speeds where configuration changes must be performed disables their ability to correct for any deviations. Pilots opted to remove this restriction, to be able to correct deviations using configuration changes, to control the speed of the aircraft as they do today.

One pilot argued that defining the time and energy boundaries up to the runway threshold does not make sense as replanning is deactivated once the aircraft is established on the glideslope. It would be more intuitive to define the boundaries from ToD to the IAF and finally to the glideslope intercept point.

Many pilots requested system improvements to prevent occasional segments of fast decelerations that required level flight. The autopilot often climbed momentarily to decelerate sufficiently as a result of SOE control. This climb was sometimes rather abrupt and pilots

were concerned about passenger comfort. In addition pilots suggested that the fidelity of the simulated autopilot should be improved.

The objective results showed that in seven out of 108 flown simulations pilots were not fully stabilized at 1,000 ft; in these simulations pilots did not complete the full landing checklist but finished it later. Pilots responded that their airline procedures allow completion of the landing checklist at 500 ft. This relaxed prerequisite was met in all 108 simulations. All pilots agreed or strongly agreed that each flown scenario was safe.

HMI FEEDBACK At the end of the experiment, pilots were asked which HMI variant they preferred. The majority of the pilots, 5 out of 9, preferred HMI variant 2; pilots commented that they preferred this variant because of the configuration timer. Some pilots, however, found the timer duration too long and requested to add an aural or flashing warning to inform them of short-term configuration actions. Moreover, since the timer estimates the start location of timer countdown, it could introduce a disturbance when this estimate is incorrect while the pilots trust the timer to be correct. Hence, removing the timer and adding an aural or flashing cue could avoid distraction and loss of attention.

One pilot indicated to prefer HMI variant 1. In his opinion, all HMI variants lack a useful representation of the speed profile, leading him to select variant 1 as it was the least ‘cluttered’. According to this pilot, the indication of upcoming speed changes on the VSD and target speed on the PFD speed-tape were insufficient in providing proper speed profile information.

All pilots appreciated the configuration cues on the ND and VSD, visualized as pseudo-waypoints. This helped them in inferring time and distance intervals between configurations and plan their actions accordingly. Only a few pilots preferred to have the configurations cues present on the speed-tape as well, others favored to remove these cues to reduce clutter. One pilot commented that the next flap ‘hook’ was not required or not even used.

Pilots preferring HMI variant 3 responded that at least they would require HMI variant 2, but also liked the TEI as it supported them in gaining ‘situation and automation awareness’. Other pilots argued, however, that the TEI was unnecessary and could be distracting with the limited energy and time deviations seen during this experiment. They also commented that the TEI could be of more use in real-life operations, when larger deviations are expected due to wind estimation errors and effects of turbulence.

Seven out of nine pilots indicated that they prefer to have an indication of every new TEMO replan. One pilot answered not to indicate every new TEMO replan, provided the algorithm successfully calculated a new plan. Another pilot indicated to be notified only of ‘considerable’ replans, that is, solving time deviations in excess of 2 seconds.

Pilots commented that the use of auto-speedbrakes is required for correct TEMO oper-

ations, as manual selection of speedbrakes would be too labor intensive in the busy TMA. However, some pilots wondered what the effect on passenger comfort and load factor would be as they could not experience this themselves in the fixed-base simulator.

Thrust and speedbrake cues were considered as nice additional features, but were also found confusing sometimes, as the text indication of thrust or speedbrakes actions was only visible for a short period. One pilot argued that these cues are not required as he/she trusts the auto-thrust and auto-speedbrake functions to work as intended.

V.C. Human vs. Autobot Comparison

The time deviations at the runway threshold are compared between piloted and Autobot runs, see Fig. 9(a). The differences were the result of, overall, more variability and also slightly later selection of configurations by pilots as compared to the Autobot.

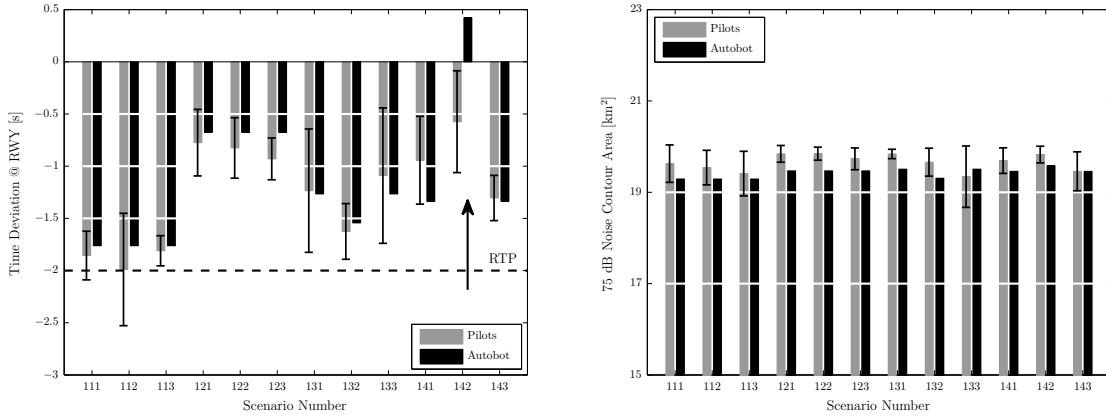
The runs flown with the Autobot do not arrive exactly on time either, however, and show a consistent offset. This offset results from deviations between the planned and the actually flown trajectories, due to modeling errors and simplifications in the TEMO algorithm. Moreover, using strategic replanning, deviations are allowed within boundaries and, hence, deviations are not absolutely minimized.⁵ Results show that even with a perfect, zero-delay pilot response, much of the allowed time deviation is already consumed by these modeling simplifications and errors. This leaves little room for additional disturbances, such as a delayed and varying pilot response.

Scenarios with an energy deviation (scenarios 121–123) force a new trajectory calculation, leading to smaller time deviations at the threshold; this corresponds with the results for piloted runs (Section V.A.1). Overall, pilots arrived slightly earlier as compared to the Autobot runs, most likely caused by delayed selection of configurations.

Analysis of the Autobot runs showed that a strong negative correlation ($\tau = -1, p < 0.001$, Kendall’s tau two-tailed) exists between the time deviation ($D(12) = 0.247, p < 0.05$) at the runway and energy deviation ($D(12) = 0.309, p < 0.05$) at glideslope intercept. Hence, without variations in selecting configurations, the time deviation is fully correlated with the energy deviation at glideslope intercept.

The largest difference between Autobot and piloted runs occurs in Scenario 142. Investigation of these runs showed that pilots require 15 seconds to enter the CTA into the FMS. Due to this delay, the aircraft predicts a different initial position for the TEMO replan. Although in absolute terms this difference is still small, this emphasizes the need to verify that TEMO is robust with respect to varying delay times in pilot actions for all relevant scenarios.

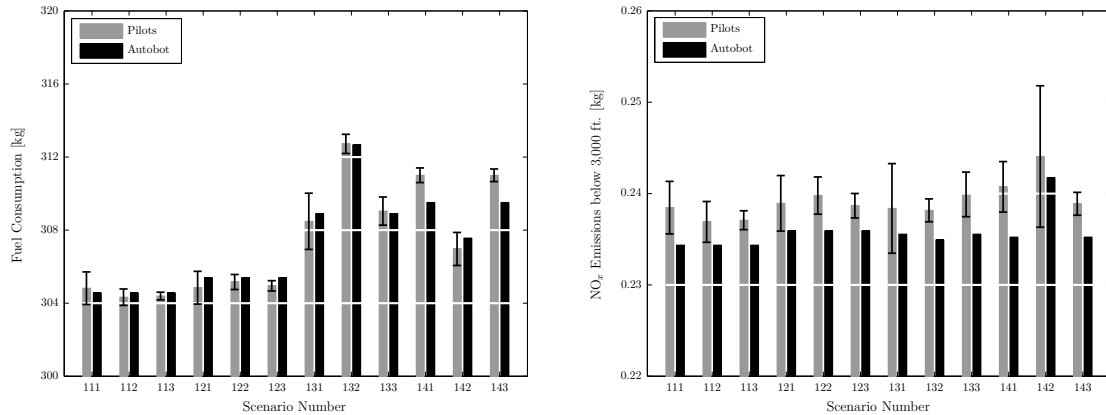
Scenario 142 shows that the Autobot arrived late while pilots, on average, arrived rather early at the runway for this scenario. This resulted from the different trajectories and strate-



(a) Comparison of time deviation at the runway threshold per scenario between piloted vs. Autobot runs. (b) Comparison of the 75 dB Noise Contour Area per scenario between piloted vs. Autobot runs.

Figure 9. Time deviation and 75 dB SEL comparison between Autobot and piloted simulations including the 95% confidence interval for the piloted simulations.

gies calculated by the algorithm at different moments in time due to the difference in entering of CTA information into the FMS. For the conditions of scenario 142, the differences in trajectories were quite large, whereas this effect was smaller for the other scenarios. Moving towards real-life operations will increase uncertainties during prediction of this initial position. Hence, it remains to be seen what the effect of these uncertainties will be on the accuracy of the calculated trajectories.



(a) Comparison of fuel consumption per scenario between piloted vs. Autobot runs. (b) Comparison of NO_x emitted below the mixing height between piloted vs. Autobot runs.

Figure 10. Fuel and NO_x comparison between Autobot and piloted simulations including the 95% confidence interval for the piloted simulations.

Fig. 9(b) compares the generated aircraft noise between the piloted and Autobot runs. On average, the piloted runs generate slightly (2%) larger 75 dB SEL contour areas. The data in Fig. 9(b) also shows that the energy disturbance at ToD results in a slightly larger

75 dB SEL contour. Interestingly, a negative CTA offset (arriving early) yields a slightly smaller contour, even though more thrust is required and more fuel is burned as shown in Fig. 10(a). This additional engine use is compensated by the reduced flight duration, which counteracts these effects and reduces the noise contour area.

Fig. 10(a) shows only small differences in fuel consumption less than 0.5%. In certain scenarios the piloted runs consumed slightly less fuel, compared to the Autobot runs, which is the result of different solutions found after replanning.

Overall, the Autobot runs yielded reduced NO_x emissions below 3,000 ft, by 2.3% compared to the piloted runs.

VI. Discussion

The data confirms the type of HMI display used does not affect the approach timing. The presence of the configuration timer in HMI variants 2 and 3 however did enable pilots to perform configuration actions more accurately. However, this had only a minor effect on the actual time of arrival at the runway threshold, supporting the Hypothesis 1 that all three HMI variants provide the necessary information to support pilots in flying TEMO descents.

Pilots commented, that they prefer to have the configuration timer present, as it supports them in selecting configurations on time. Some pilots suggested to replace the visual timer with an aural cue, to avoid distraction. Overall, HMI 2 was the preferred HMI, confirming Hypothesis 2. Pilots responded that in the limited scope of this experiment, the Time and Energy Indicator (HMI variant 3) is not required, but that it could be useful in real-life operations with larger disturbances.

TEMO requires configuration changes to be performed at fixed nominal speeds, as research³⁹ indicated the risk of increased wear if flaps are used to control aircraft speed. Pilots found the configuration changes manageable, yet strict, and they would prefer the ability to deviate from the commanded configuration changes to correct time deviations when descending on the glideslope. This yields a degree of freedom on the glideslope without using thrust or speedbrakes as pilots could add drag to reduce airspeed when flying faster than originally planned. Conversely, postponing selections could help the aircraft to gain time.

Regarding the acceptability of the procedures (Hypothesis 3), pilots responded that the strict and accurate selection of configurations can not be achieved in real-life operations. Therefore, the TEMO concept should be revised to allow dynamic configuration changes for closed-loop control during descent down the glideslope. This reduces the need for strict selection of configurations as such variations can be corrected using the next configuration selection. For pilot support, a closed-loop flap-scheduling algorithm^{39,40} could be used, but then including maximum configuration extension speeds to reduce flap wear. Flap-scheduling

would also reduce the need for a configuration timer, as our data showed that the accuracy of the timer in estimating the timer start location is still limited, due to speed and energy deviations during timer countdown.

Although timing differences between the nominal Autobot runs and piloted runs are small, there are differences in fuel burn, noise and emissions, leading to rejection of Hypothesis 4. More generally, the timing performance reached is thus not uniquely linked to the fuel burn and emissions.

The performance data also showed that the energy deviation at the glideslope intercept point significantly affects the time of arrival for the Autobot runs, while for the piloted runs this effect was smaller due to variations in pilot response. Time deviations occur due to modeling errors in the planned trajectory and are inherent to strategic replanning, which allows deviations from the planned trajectory within boundaries. Reducing these deviations by enhanced modeling is limited to what we know of our environment⁴¹ and is likely to extend replan calculation times. The deviation boundaries could therefore be constricted to reduce the allowed deviations, while the glideslope intercept guidance could be enhanced to simultaneously intercept the glideslope whilst following the speed profile using thrust or speedbrakes.

Since replanning is disabled after glideslope intercept, the aircraft descends for an extended period during which deviations can occur and grow that are not corrected. Moving TEMO towards real-life operations will introduce more uncertainties than currently modeled. Aircraft mass, engine dynamics and wind will continuously disturb a TEMO descent. Hence, if strict time accuracies are required, sustained deviations and errors should be minimized, even on the glideslope. However, replans were often unsuccessful on the glideslope and close to the runway. For this reason, a different strategy is required to correct deviations during final descent to ‘close-the-loop’.

The TEMO system could be closed using automation or the pilot. Using a tactical control-law, automation supports the system to minimize deviations by continuously correcting deviations. This can be achieved by continuously changing the speed profile⁵ or through flap-scheduling.^{39,40} Alternatively, the role of the supervising pilot could be increased by using flaps to control aircraft speed and by monitoring deviations to negotiate new constraints with ATC when required and possible. However, both solutions introduce new human-machine coordination issues that require further investigation.

VII. Conclusions

Time and Energy Managed Operations (TEMO) was tested in a pilot-in-the-loop simulation study to evaluate the conceptual procedures and display support required by pilots to

perform TEMO operations. Three different display variants were tested; a minimal display, showing only configuration cue information, a display extended with a configuration timer and notifications on the functioning of the TEMO algorithm, and an extended display with time and energy indication. Pilots commented that the procedures were clear and preferred the HMI variants which included a configuration timer. There were no observed differences in approach timing performance using any of the three displays that were evaluated. This was confirmed by a comparison between piloted responses and automated, zero-delay responses, which showed little effect of response variations on environmental impact and approach timing. Differences in time deviations in piloted versus automated runs are small, suggesting that the time deviations found are mainly caused by imperfections in TEMO's planning and guidance algorithms. Pilots responded that the requirement of accurate selection of configuration changes is too strict and would appreciate more flexibility in deviating from planned selection points. In addition, when the required accuracy of 2 seconds is necessary, future research should address the final approach segment. In the current concept replanning is disabled during that segment, and consequently the largest remaining time deviations occur there.

Acknowledgments

The research leading to these results received funding from the European Union's Seventh Framework Programme (FP7/2007-2013) through the Clean Sky Joint Technology Initiative under Grant Agreement no. CSJU-GAM-SGO-2008-001.

The authors acknowledge the contributions of M.M. Heiligers, G. Temme, W. Huson, V. Steinmetz and J. Ertzgaard of the NOCONDES consortium during preparation and execution of this experiment. Furthermore, J. Groeneweg, B. Heesbeen, A. Marsman and M. Valens (all NLR) and C. Borst (TU Delft) are acknowledged. Much appreciation goes out to all pilots that participated in the experiment.

References

¹EUROCONTROL, "Long-Term Forecast: IFR Flight Movements 2010-2030," Tech. Rep. CND/STATFOR Doc415, EUROCONTROL, Dec. 2010.

²NextGen Office, "FAA's NextGen Implementation Plan 2012," Tech. rep., FAA, 800 Independence Avenue, Washington (DC), March 2012.

³SESAR, "European ATM Master Plan," Tech. Rep. Edition 2, EUROCONTROL, Oct. 2012, SESAR JU & SESAR Work Package C and Partners.

⁴ICAO, *Continuous Descent Operations (CDO) Manual - Doc 9931 AN/476*, International Civil Aviation Organization, Montreal, Canada, 2010.

⁵De Jong, P. M. A., De Gelder, N., Bussink, F. J. L., Verhoeven, R. P. M., Kohrs, R., Van Paassen, M. M., and Mulder, M., “Time and Energy Management during Descent and Approach: Batch-Simulation Study,” *Journal of Aircraft*, Vol. 52, No. 1, 2015, pp. 190–203.

⁶Williams, D. H., Oseguera-Lohr, R. M., and Lewis, E. T., “Design and Testing of a Low Noise Flight Guidance Concept,” Technical Memorandum NASA/TM-2004-213516, National Aeronautics and Space Administration, Langley Research Center, Hampton (VA) 23681-2199, Dec. 2004.

⁷Oseguera-Lohr, R. M., Williams, D. H., and Lewis, E. T., “Crew Procedures for Continuous Descent Arrivals Using Conventional Guidance,” Technical Memorandum NASA/TM-2007-214538, National Aeronautics and Space Administration, Langley Research Center, Hampton (VA) 23681-2199, Febr. 2007.

⁸Klooster, J. K., Wickman, K. D., and Bleeker, O. F., “4D Trajectory and Time-of-Arrival Control to Enable Continuous Descent Arrivals,” *Proc. of the AIAA Guidance, Navigation and Control Conference and Exhibit, Honolulu (HI), Aug. 18–21*, No. AIAA 2008-7402, American Institute of Aeronautics and Astronautics, 2008, pp. 1–17.

⁹Garrido-López, D., D’Alto, L., and Gomez Ledesma, R., “A Novel Four-Dimensional Guidance for Continuous Descent Approaches,” *Proc. of the 28th Digital Avionics Systems Conference, Orlando (FL), Oct. 23–29*, IEEE/AIAA, 2009, pp. 6.E.1–1–6.E.1–11.

¹⁰De Prins, J. L. and Gomez Ledesma, R., “Towards Time-based Continuous Descent Operations with Mixed 4D FMS Equipment,” *Proc. of the 11th AIAA Aviation Technology, Integration, and Operations (ATIO) Conference (VA) Beach (VA), Sept. 20–22*, No. AIAA 2011-7018, American Institute of Aeronautics and Astronautics, 2011, pp. 1–18.

¹¹Williams, D. H., Oseguera-Lohr, R. M., and Lewis, E. T., “Energy Navigation: Simulation Evaluation and Benefit Analysis,” Technical Publication NASA/TP-2011-217167, National Aeronautics and Space Administration, Langley Research Center, Hampton (VA) 23681-2199, Aug. 2011.

¹²Park, S. G. and Clarke, J.-P. B., “Vertical Trajectory Optimization for Continuous Descent Arrival Procedure,” *Proc. of the AIAA Guidance, Navigation and Control Conference, Minneapolis (MI), Aug. 13–16*, No. AIAA 2012-4757, American Institute of Aeronautics and Astronautics, 2012, pp. 1–19.

¹³Amelink, M. H. J., Mulder, M., Van Paassen, M. M., and Flach, J. M., “Theoretical Foundations for a Total Energy-Based Perspective Flight-Path Display,” *The International Journal of Aviation Psychology*, Vol. 15 (3), 2005, pp. 205–231.

¹⁴Endsley, M. R., “Automation and Situation Awareness,” *Automation and Human Performance: Theory and Applications*, edited by R. Parasuraman and M. Mouloua, Lawrence Erlbaum Associates, Inc., Mahway (NJ), 1996, pp. 163–181.

¹⁵Billings, C. E., *Aviation Automation: The Search for a Human-Centered Approach*, Lawrence Erlbaum Associates, Inc., Mahway (NJ), 1997.

¹⁶Parasuraman, R., Sheridan, T. B., and Wickens, C. D., “A Model for Types and Levels of Human Interaction with Automation,” *IEEE Transactions on Systems, Man and Cybernetics, Part A*, Vol. 30, No. 3, May 2000, pp. 286–297.

¹⁷Dekker, S. W. A., “On the other side of promise: what should we automate today?” *Human Factors for Civil Flight Deck Design*, edited by D. Harris, chap. 8, Ashgate Publishing Limited, 2004, pp. 183–198.

¹⁸Bainbridge, L., “Ironies of Automation,” *Automatica*, Vol. 19, No. 6, 1983, pp. 775–779.

¹⁹Vicente, K. J. and Rasmussen, J., “Ecological Interface Design: Theoretical Foundations,” *IEEE Transactions on Systems, Man, and Cybernetics*, Vol. 22, No. 4, July/Aug. 1992, pp. 589–606.

²⁰Christoffersen, K. and Woods, D. D., “How to Make Automated Teams Team Players,” *Advances in Human Performance and Cognitive Engineering Research*, edited by E. Salas, Vol. 2, JAI Press/Elsevier, 2002, pp. 1–12.

²¹Abbot, T. S., “A Brief History of Airborne Self-Spacing Concepts,” Contractor Report NASA/CR–2009-215695, National Aeronautics and Space Administration, Langley Research Center, Hampton (VA) 23681-2199, Febr. 2009.

²²Verhoeven, R. P. M., “Pseudospectral aircraft descent trajectory optimization: An initial implementation,” Contract Report NLR-CR-2012-378, National Aerospace Laboratory, Amsterdam, The Netherlands, 2012.

²³Becerra, V. M., “Solving complex optimal control problems at no cost with PSOPT,” *Proc. of the IEEE International Symposium on Computer-Aided Control System Design (CACSD), Yokohama, Japan, 8–10 Sept.*, 2010, pp. 1391–1396.

²⁴“IPOPT, Interior Point OPTimizer,” Dec. 2012, <https://projects.coin-or.org/Ipopt/wiki>.

²⁵“ADOL-C, Automatic Differentiation by Overloading C++,” Dec. 2012, <https://projects.coinor.org/ADOL-C>.

²⁶Muresean, S., “Initial 4D - 4D Trajectory Data Link (4DTRAD) - Concept of Operations,” Tech. rep., EUROCONTROL, Brussels, Belgium, Dec. 2008.

²⁷Borst, C., Mulder, M., and Van Paassen, M. M., “Design and Simulator Evaluation of an Ecological Synthetic Vision Display,” *Journal of Guidance, Control and Dynamics*, Vol. 33, No. 5, Sept.–Oct. 2010, pp. 1577–1591.

²⁸Ellerbroek, J., Visser, M., Van Dam, S. B. J., Mulder, M., and Van Paassen, M. M., “Design of an Airborne Three-Dimensional Separation Assistance Display,” *IEEE Transactions on Systems, Man, and Cybernetics, part A: Systems and Humans*, Vol. 41, No. 6, 2011, pp. 863–875.

²⁹Vèque, S., “A318 - Steep Approach Operation,” Presentation at OLM FBW 2006, Toulouse, France, Sept. 2006.

³⁰Smith, P., “Date with the Eight,” *Flight International*, Vol. 182, No. 5370, 11–17 Dec. 2012, pp. 26–35.

³¹Smaili, H., Laban, M., and Dominicus, J., “New Integrated Modeling and Simulation Techniques for Research and Training Applications,” *Proc. of the AIAA Modeling and Simulation Technologies Conference and Exhibit, San Francisco (CA), 15–18 Aug.*, No. AIAA 2005-6294, American Institute of Aeronautics and Astronautics, 2005, pp. 1–17.

³²Zijlstra, F. R. H., *Efficiency in Work Behaviour: A Design Approach for Modern Tools*, Ph.D. thesis, Delft University of Technology, 1993.

³³Hart, S. G. and Staveland, L. E., “Development of NASA-TLX (Task Load Index): Results of Empirical and Theoretical Research,” *Human Mental Workload (Advances in Psychology)*, Vol. 52, 1988, pp. 139–183.

³⁴Lee, K. K. and Davis, T. J., “The Development of the Final Approach Spacing Tool (FAST): A Cooperative Controller-Engineer Design Approach,” Tech. Rep. NASA Technical Memorandum 110359, National Aeronautics and Space Administration, Aug. 1995.

³⁵“Standard Method of Computing Noise Contours around Civil Airports,” Tech. Rep. Document 29, ECAC.CEAC, Dec. 2005, 3rd Edition, Volume 1.

³⁶Martin, R. L., Oncina, C. A., and Zeeben, J. P., “A simplified method for estimating aircraft engine emissions,” *Scheduled Civil Aircraft Emission Inventories for 1992: Database Development and Analysis - NASA Contractor Report 4700, April 1996*, edited by S. L. Baughcum, T. G. Tritz, S. C. Henderson, and

D. C. Pickett, National Aeronautics and Space Administration, 1995, pp. D1–D11, Reported as “Boeing Method 2” fuel flow methodology description in Appendix D.

³⁷Field, A., *Discovering Statistics using SPSS*, SAGE Publications Ltd, 1 Oliver’s Yard, 55 City Road, London EC1Y 1SP, 2009.

³⁸Zar, J. H., *Biostatistical Analysis*, Prentice Hall, Inc., Upper Saddle River (NJ), 5th ed., 2010.

³⁹De Leege, A. M. P., In ’t Veld, A. C., Mulder, M., and Van Paassen, M. M., “Three-Degree Decelerating Approaches in High Density Arrival Streams,” *Journal of Aircraft*, Vol. 46, No. 5, 2009, pp. 1681–1691.

⁴⁰De Jong, P. M. A., In ’t Veld, A. C., De Leege, A. M. P., Van Paassen, M. M., and Mulder, M., “Control Space Analysis of Three-Degree Decelerating Approaches at Amsterdam Airport Schiphol,” *Proc. of the AIAA Guidance, Navigation and Control Conference, Toronto, Canada, Aug. 2–5*, No. AIAA 2010-8454, American Institute of Aeronautics and Astronautics, 2010, pp. 1–20.

⁴¹Sheridan, T. B., *Telerobotics, Automation, and Human Supervisory Control*, MIT Press, Cambridge (MA), 1992.